Discover Oncology

Research

Exploring the prognosis value, immune correlation, and drug responsiveness prediction of homeobox C6 (HOXC6) in lung adenocarcinoma

Mei Xin[1] · Huajian Peng[2] · Linbo Zhang[1]

© The Author(s) 2024   OPEN

Abstract

Backgrounds Homeobox C6 (HOXC6) is a gene that encodes for a transcription factor involved in various cellular processes, including development and differentiation, and regulates cancer progression. However, the carcinogenesis and effect of HOXC6 in lung adenocarcinoma (LUAD) still need further investigation.

Methods The differential HOXC6 expression levels at the mRNA and protein level were explored in multiple public datasets, including The Cancer Genome Atlas (TCGA) and Human Protein Atlas (HPA) dataset. Gene Expression Omnibus (GSE31210), International Cancer Genome Consortium (ICGC) datasets and the LUAD sample from Affiliated Hospital of Guangxi Medical University. We also investigated the relation between HOXC6 expression and clinicopathologic indexes. Furthermore, the correlation of immune infiltration, drug responsiveness and HOXC6 were explored.

Results The upregulated HOXC6 expressions at mRNA and protein levels were found in LUAD tissues compared to the normal lung tissues. Besides, the relatively shorter overall survival time, worse T and N stages, and lower immune scores were found in the high-expression HOXC6 subgroup. Notably, T cells regulatory (Tregs), Macrophages M0, and Plasma cells had the higher infiltration levels in the high-HOXC6 expression subgroup, while NK cells activated, Monocytes, Dendritic cells resting, and Mast cells resting had the lower infiltration levels. In drug sensitivity analysis, we revealed that LUAD patients with high-HOXC6 expression may be more susceptible to Camptothecin, Cytarabine, Docetaxel, Elesclomol, Rapamycin, Sorafinib, Temsirolimus, and Vorinostat.

Conclusions Taken together, there is a great potential for HOXC6 to become a prognosis biomarker and contribute to develop treatment strategies for LUAD patients. Further mechanism exploration and drug development for HOXC6 are needed.

Keywords Homeobox C6 · Lung adenocarcinoma · Clinicopathologic correlation · Bioinformatics · Immune filtration · Treatment response

---

Mei Xin, Huajian Peng contributed to the work equally and should be regarded as co-first authors.

✉ Linbo Zhang, zhanglinbo@gxmu.edu.cn; Mei Xin, 31532567@qq.com; Huajian Peng, penghuajian@ stu.gxmu.edu.cn | ¹Department of Health Management, The First Affiliated Hospital of Guangxi Medical University, Nanning 530021, People's Republic of China. ²Department of Thoracic Surgery, The First Affiliated Hospital of Guangxi Medical University, Nanning 530021, People's Republic of China.

Discover

1 Introduction

It was projected that, in 2020, there will be 1.8 million lung cancer-related fatalities and 2.2 million additional incidences of lung malignancy which is the second most prevalent cause of cancer-related death in women and the top cause of cancer-related death in men worldwide [1, 2]. Nearly forty percent of all lung malignancies are lung adenocarcinomas (LUAD) which develops from glandular cells and is one of the most prevalent kinds. The contributing factors of LUAD contains smoking, exposure to environmental harmful substances, previously present respiratory disorders, and inherited and molecular mechanisms.

Being a member of the homeobox gene family, Homeobox C6 (HOXC6) contributes to transcription elements encoding and cellular proliferation and differentiation. It has been proposed that in multiple kinds of solid cancers, such as prostate, lung, and gastrointestinal malignancies, HOXC6 could regulate a number of biological functions, including cell proliferation, survival, and metastasis [3–7]. The activation of mammalian target of rapamycin (mTOR) pathway resulting from HOXC6-related PPP2R2B repression and HOXC6-induced Mitogen- and stress-activated kinase up-regulation which carried the ability to inhibit apoptosis promoted the proliferation of Pancreatic ductal adenocarcinoma [8]. Utilizing a particular gene code containing HOXC6, HOXC8 and HOXB7, Steens J et al., manage to induce human skin fibroblasts to directly convert into Mesenchymal stem cells (MSCs) which is an appealing focus for cell fate conversion. Moreover, these transformed cells with MSCs characteristics can secrete cytokines contributing to tissue repair and immune regulation [9]. With regard to lung cancer, the upregulated HOXC6 expression levels have been revealed in non-small cell lung cancer (NSCLC) tissues and were connected to cancer development and progress [4].

However, for LUAD, a common type of lung cancer, exploring an underlying carcinogenic mechanism and clinical guidance of HOXC6 makes sense. In this project, utilizing multiple public databases and the LUAD samples from our hospital, deregulated HOXC6 expression level in LUAD tissue was tried to be verified. Furthermore, we aimed to uncover the prognostic value, immune correlation, and drug response projection of HOXC6.

2 Materials and methods

2.1 Data source

The transcriptome sequencing and genetic mutation data for LUAD patients were acquired from The Cancer Genome Atlas (TCGA) database (Workflow Type: TPM; https://portal.gdc.cancer.gov/repository), and corresponding clinicopathologic info, including gender, age, American Joint Committee on Cancer (AJCC) pathologic stage, was originated from UCSC xena online program (https://xena.ucsc.edu/). As the validation set, GSE31210 dataset including the gene expression profiling and overall survival (OS) info of 227 LUAD patients and ICGC-LUAD dataset including the gene expression profiling were retrieved from Gene Expression Omnibus (GEO) (https://www.ncbi.nlm.nih.gov/geo/) and International Cancer Genome Consortium (ICGC; http://dcc.icgc.org) databases respectively. Besides, the 16 pairs LUAD and corresponding adjacent normal lung tissue samples for quantitative polymerase chain reaction (PCR) and the other 12 pairs for immunohistochemistry (IHC) from the First Affiliated Hospital of Guangxi Medical University served as the GX-LUAD cohort. The previously published procedures for tissue storage, RNA extraction, and quantitative PCR for reverse transcription were followed [10]. The designed sequence info of PCR primer is listed as below: GAPDH, forward: GTCAGCCGCATCTTC TTT, reverse: CGCCCAATACGACCAAAT. *HOXC6*, forward: AGACGAGAAAGAGAGTGGGAGA, reverse: GCTGGAACTGAACAC GACATTCT. Moreover, the expression of HOXC6 was determined employing 2 ΔΔCT methodology [11].

2.2 Exploring the differential expression and prognostics value of HOXC6 in LUAD

The HOXC6 expression levels were compared between LUAD and normal or neighboring lung tissues in the TCGA-LUAD, ICGC-LUAD and Guangxi cohorts respectively. In addition, the Human Protein Atlas (HPA) database (https://www.proteinatlas.org) was applied to reveal the HOXC6 expression at a protein level in LUAD and normal lung tissues. In the survival analysis, we applied the "survival" and "survminer" R packages to obtain the optimized cut-off value of HOXC6-expression level for prognostic value evaluation. Then, high- and low-HOXC6 expression subgroups were categorized by cut-off value of HOXC6 expression. Kaplan–Meier survival plots for OS were depicted between two subgroups in the TCGA-LUAD and GSE31210 cohorts. Employing the R packages "ggpubr" and "limma", the differences in HOXC6 expression levels across

various clinicopathological characteristics were examined in the TCGA-LUAD cohort and the results were illustrated as boxplot and heatmap.

To validate the protein expression level of HOXC6 in tumor tissue, we further performed the immunohistochemistry (IHC) of the 12 pairs LUAD and corresponding adjacent normal lung tissue samples in the Guangxi cohort. The paraffin section, staining and quantitative evaluation procedures of IHC was previously described [12, 13]. As directed by the manufacturer, all primary antibodies were diluted and incubated for the entire night at 4 °C. The following primary antibodies were employed in this investigation: HOXC6 (1:200, Bioss, China).

2.3 Nomogram construction

Adopting a multivariate Cox proportional risk regression model in "survival" and "rms" R packages [14, 15], the nomogram relying on the TCGA-LUAD data was developed to project the probabilities of 1-, 3-, and 5-year OS. The LUAD patients with insufficient clinicopathological info were eliminated. This prediction model combined HOXC6 expression with clinicopathological indicators, including gender, age, AJCC pathologic Tumor Node Metastasis (TNM) stage, which are routinely available in our clinical practice. The consistency levels of 1-, 3-, and 5-year calibration curves were utilized to evaluate the discrimination efficiency of nomogram.

2.4 Gene expression and TMB correlation analysis of HOXC6

Based on the transcriptome profile of TCGA-LUAD at mRNA level, the Pearson correlation analyses were performed to discover HOXC6-related genes. Top 10 HOXC6-related genes were identified under specific situations that the cut-off value of correlation coefficient was set to 0.6 and *P*-value was set to 0.001. The above comprehensive results were summarized in a circus plot. Moreover, Pearson correlation analyses were further performed to disclose the relationships between HOXC6 and the genes associated with immune checkpoints, including IDO1, LAG3, CTLA4, TNFRSF9, ICOS, CD80, PDCD1LG2, TIGIT, CD70, TNFSF9, ICOSLG, KIR3DL1, CD86, PDCD1, LAIR1, TNFRSF8, TNFSF15, TNFRSF14, IDO2, CD276, CD40, TNFRSF4, TNFSF14, HHLA2, CD244, CD274, HAVCR2, CD27, BTLA, LGALS9, TMIGD2, CD28, CD48, TNFRSF25, CD40LG, ADORA2A, VTCN1, CD160, CD44, TNFSF18, TNFRSF18, BTNL2, C10orf54, CD200R1, TNFSF4, CD200, and NRP1. Tumor mutation burden (TMB) makes a difference in predicting prognosis and immunotherapy response for LUAD patient [16]. We summarized the genetic mutation data of TCGA-LUAD and the TMB of each tumor sample was worked out. Then, the spearman correlation was implemented between the TMB value and HOXC6 expression.

2.5 GSEA function enrichment analysis

Based on TCGA-LUAD dataset, the Gene Set Enrichment Analysis (GSEA) was carried out between the low- and high-*HOXC6* expression subgroups to identify the possible regulating pathways of HOXC6, in which R package, including "org. Hs.eg.db" and "clusterProfiler" and the gene set data, including "c2.all.v7.0.symbols.gmt" and "c5.all.v7.0.symbols.gmt" were employed [17]. Relevant enrichment pathways were determined by functional terms that satisfied the requirements of a nominal $P < 0.05$ and a false discovery rate (FDR) < 0.25. Then, the top 7 pathways with the smaller *P*-value were visualized.

2.6 Immune cell infiltration analysis

Cell-type identification by estimating relative subsets of RNA transcripts (CIBERSORT) is a novel analytical methodology to estimate the relative abundance of different immune cell types in tumor utilizing gene expression data [18]. Using CIBERSORT (R script v1.03), the proportions of various immune cells were assessed for each tumor sample based on the TCGA-LUAD gene expression profiling. Then, to uncover the correlation between HOXC6 and tumor immune infiltration, Spearman correlation analyses and relative abundance difference analysis were conducted. Additionally, employing "estimate" R package and reference data, including "commonGenes.gct" and "estimateScore.gct", the stromal score, immune score and ESTIMATE (Estimation of Stromal and Immune cells in Malignant Tumor tissues using Expression data) score of each TCGA-LUAD samples were calculated [19]. And we further explored whether there was a difference in these scores between the low- and high-HOXC6 expression subgroups.

Discover

2.7 Drug sensitivity prediction analysis

In the drug sensitivity assessment study, the "pRRophetic" R package was adopted to estimate the half-maximal inhibitory concentrations (IC50s) of TCGA-LUAD cohort to chemotherapeutic and targeted medicines linked to LUAD managements by ridge regression method [20]. In addition, The Cancer Immunome Atlas (TCIA, https://tcia.at/) online program provides the immunophenotypic score (IPS) of a tumor sample using the transcriptome info of solid cancers from TCGA dataset. To some extent, the therapeutic responsiveness to immune-checkpoint inhibitors (ICIs), including anti-programmed cell death protein 1 (PD-1) and anti- cytotoxic T lymphocyte antigen-4 (CTLA-4) antibodies, could be reflected in IPS value [21]. A higher IPS suggests a possibly finer reaction to immunotherapy. Next, we further probed into the differences of IC50s and IPS in the low- and high-HOXC6 expression subgroups in the TCGA-LUAD cohort.

2.8 Statistical analysis

The data analysis and result visualization were performed using R (v4.3.1). For continuous data, the Wilcoxon rank-sum test was utilized to compare data between various subgroups, whereas for categorical data, the chi-square test was applied. The difference in HOXC6 expression levels between the LUAD and the accordingly neighboring normal tissues of the TCGA and GX-LUAD cohorts was investigated using a paired t-test. $P < 0.05$ was given as the threshold if not specifically mentioned.

3 Results

3.1 The upregulated expression level of HOXC6 in LUAD

The TCGA-LUAD tissues exhibited a notably higher level of HOXC6 mRNA expression (Fig. 1A, B). The elevated HOXC6 expressions in LUAD tissues were further verified in the GEPIA online program, ICGC- and GX-LUAD cohorts (Fig. 1C–E). Using HPA online program, the HOXC6 expression at a protein level in LUAD and normal lung tissues were observed (Figure S1A–F). According to the IHC, the representative IHC images of two LUAD patients were exhibited (Fig. 1I–J), and the semi-quantitative IHC scoring demonstrated that the higher protein expression levels of HOXC6 were observed in the LUAD tissues compared to the corresponding adjacent lung tissues (Fig. 1K).

3.2 HOXC6 correlated with dismal overall survival and poor clinical stage

In the TCGA-LUAD dataset, a total of 463 LUAD patients with according OS info were included. Using the OS-oriented method, the HOXC6 expression value of a cutoff that corresponded to the most significant relation with OS was calculated in the TCGA-LUAD cohort (Fig. 1F). The Kaplan Meier survival analysis revealed that the LUAD patients in the high HOXC6-expression group carried a worse OS in the TCGA cohort (Fig. 1G). Furthermore, the dismal prognosis of the high HOXC6-expression subgroup was validated in the GSE31210 cohorts (Fig. 1H). Moreover, higher upregulated HOXC6 level was shown in the TCGA-LUAD patients with more advanced clinical stage (AJCC pathologic T2 and T3 vs. T1, Fig. 2A) and more progressed lymph node metastasis (N1 vs. N0, Fig. 2B). Nevertheless, the differences of HOXC6 expression between different AJCC pathologic stages, genders, ages, and pathologic M stages were not observed (Fig. 2C–F). In heatmap, we described the distribution of TCGA-LUAD patients with different clinicopathological traits between the high- and low- HOXC6 expression subgroups and found that the AJCC pathologic T staging was discrepant (Fig. 2G).

3.3 Construction of a nomogram to project overall survival

Based on the constructed nomogram, we can predict the 1-, 3-, and 5-year OS of LUAD patient by integrating the HOXC6 expression with readily available clinicopathological traits in clinical practice (Fig. 3A). As a test of the
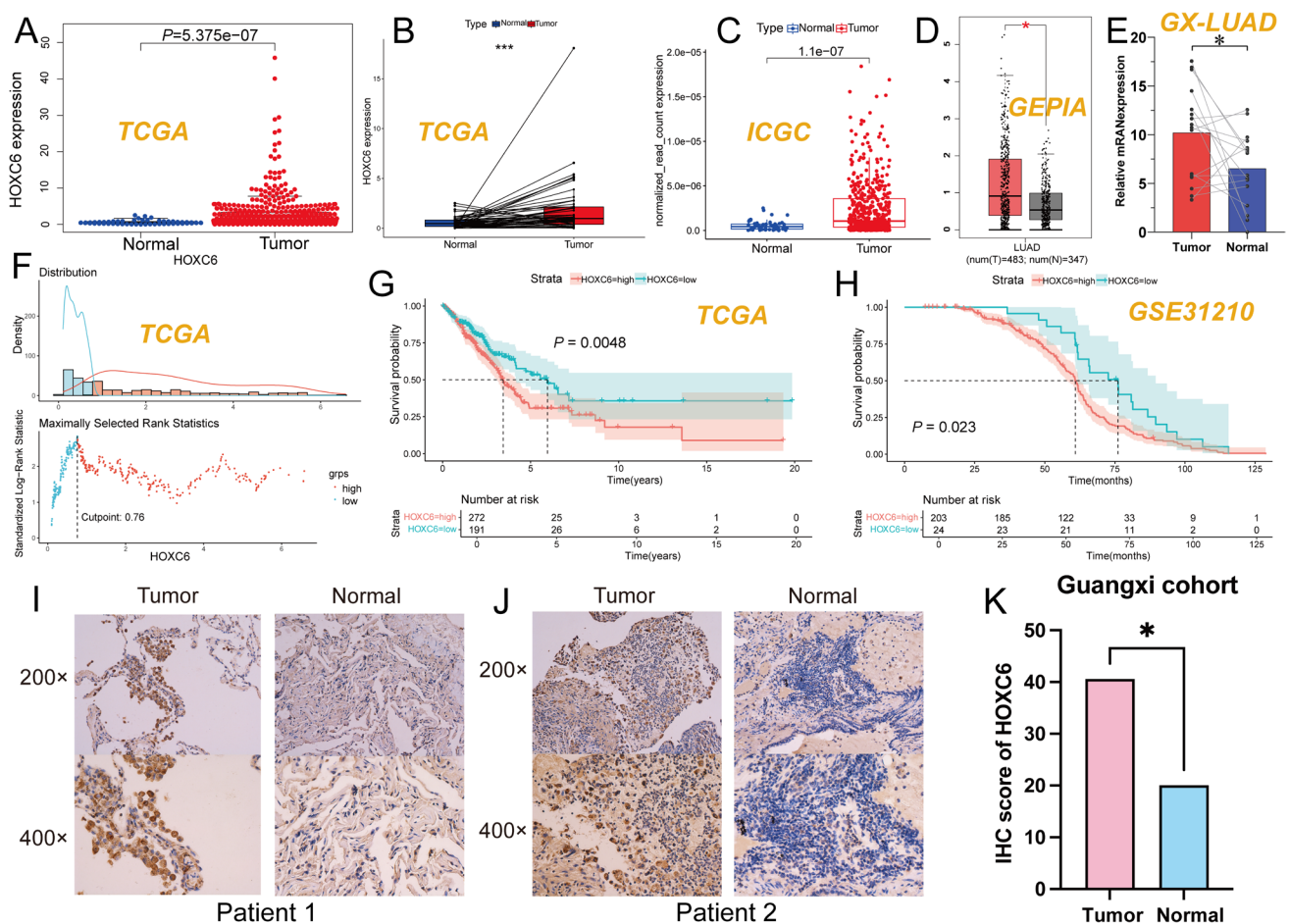
Fig. 1 A, **B** Scatter plots illustrated a notably higher level of HOXC6 mRNA expression in LUAD tissues compared with normal or adjacent lung tissues in the TCGA-LUAD cohorts. **C–E** The elevated HOXC6 expressions in LUAD tissues were further verified in the GEPIA online program, ICGC- and GX-LUAD cohorts. **F** The cutoff of HOXC6 expression that corresponded to the most significant relation with OS was calculated in the TCGA-LUAD cohort. **G**, **H** The Kaplan Meier survival plots demonstrated that the LUAD patients in the high HOXC6-expression group carried a worse OS in the TCGA and GSE31210 cohorts. **I–J** IHC images of HOXC6 in the LUAD and adjacent lung tissues of two LUAD patients. **K** Bar chart of IHC scores for HOXC6 in the 12 pair LUAD and adjacent lung tissues. HOXC6, Homeobox C6; LUAD, Lung Adenocarcinoma; TCGA, The Cancer Genome Atlas; GEPIA, Gene Expression Profiling Interactive Analysis; ICGC, International Cancer Genome Consortium; OS, overall survival; IHC, Immunohistochemistry. *$P < 0.05$; **$P < 0.01$

nomogram, the calibration curves illustrated an acceptable degree of coherence between the projected and the actual OS rates at 1, 3, and 5 years (Fig. 3B).

3.4 Up-regulated HOXC6 may be involved in *cancer*-promoting and cell cycle related pathways

The enrichment analysis for GO terms revealed the significant relationships between HOXC6 up-regulation and multiple pathways, including "GOBP_DETECTION_OF_CHEMICAL_STIMULUS, GOMF_OLFACTORY_RECEPTOR_ACTIVITY, and GOBP_SENSORY_PERCEPTION_OF_SMELL" pathways, while low HOXC6 expression related to "GOMF_RNA_POLY-MERASE_CORE_ENZYME_BINDING, GOMF_BASAL_TRANSCRIPTION_MACHINERY_BINDING, GOMF_RNA_POLYMER-ASE_BINDING, and GOBP_REGULATION_OF_GENE_SILENCING" pathways (Figure S2A). Moreover, KEGG enrichment analysis demonstrated that "KEGG_DRUG_METABOLISM_OTHER_ENZYMES, KEGG_MATURITY_ONSET_DIABETES_OF_THE_YOUNG, KEGG_OLFACTORY_TRANSDUCTION, KEGG_PENTOSE_AND_GLUCURONATE_INTERCONVERSIONS, KEGG_PORPHYRIN_AND_CHLOROPHYLL_METABOLISM, KEGG_STARCH_AND_SUCROSE_METABOLISM, and KEGG_STEROID_HORMONE_BIOSYNTHESIS" pathways were enriched in the up-regulated HOXC6 subgroup (Figure S2B).
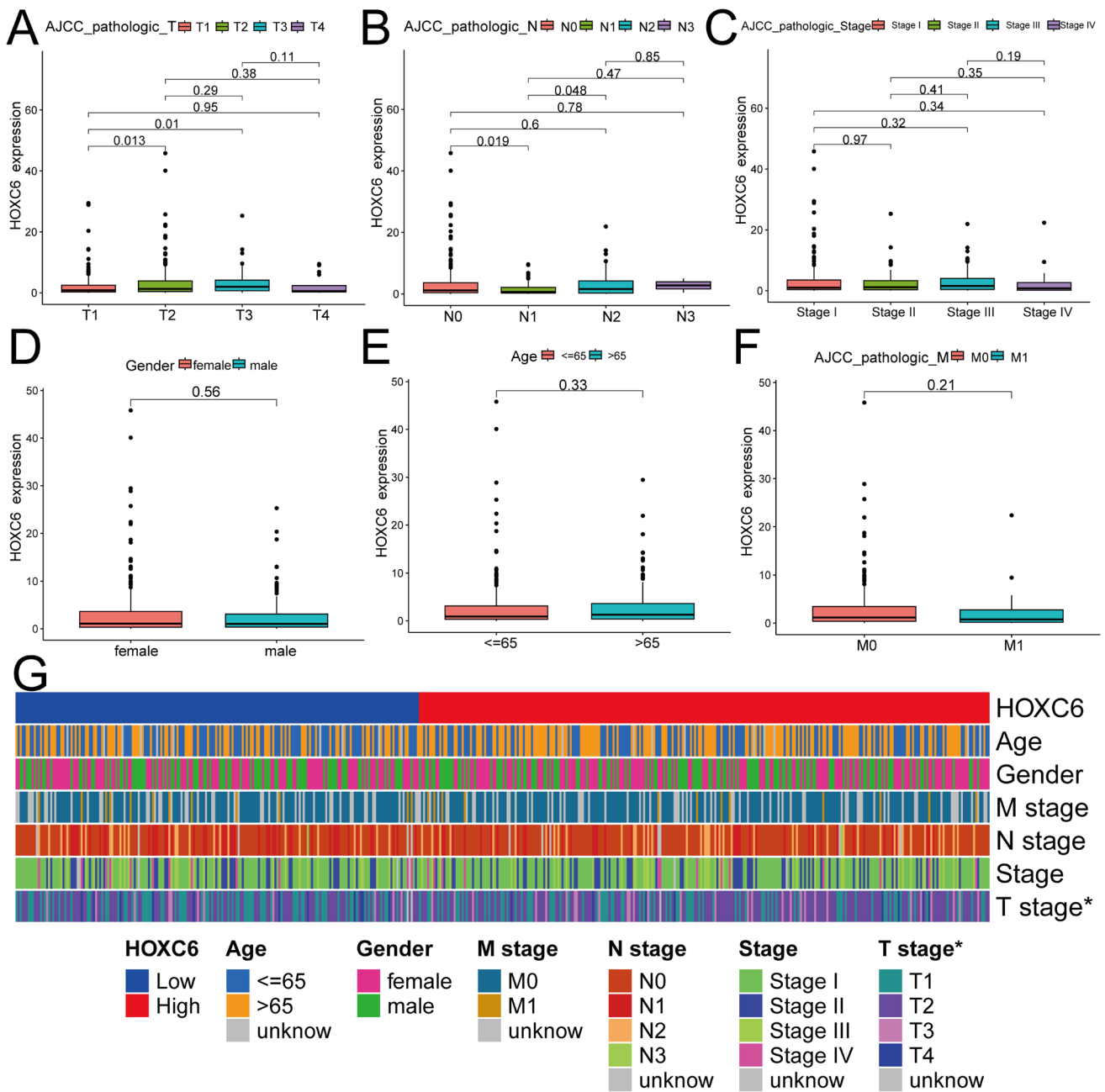
Fig. 2 A–F The HOXC6 expression level was compared in the different clinicopathological characteristics, including AJCC pathologic T stage, AJCC pathologic N stage, AJCC pathologic stage, gen-der, age, and pathologic M stage, in the TCGA-LUAD patients. **G** The heatmap illus-trated the differences in HOXC6 expression levels across various clinicopathological characteristics. HOXC6, Homeobox C6; LUAD, Lung Ade-nocarcinoma; TCGA, The Cancer Genome Atlas; TNM, Tumor Node Metastasis; AJCC, American Joint Committee on Cancer

3.5 HOXC6 was associated with some HOX family genes, immune checkpoint-related genes, and tumor mutation burden
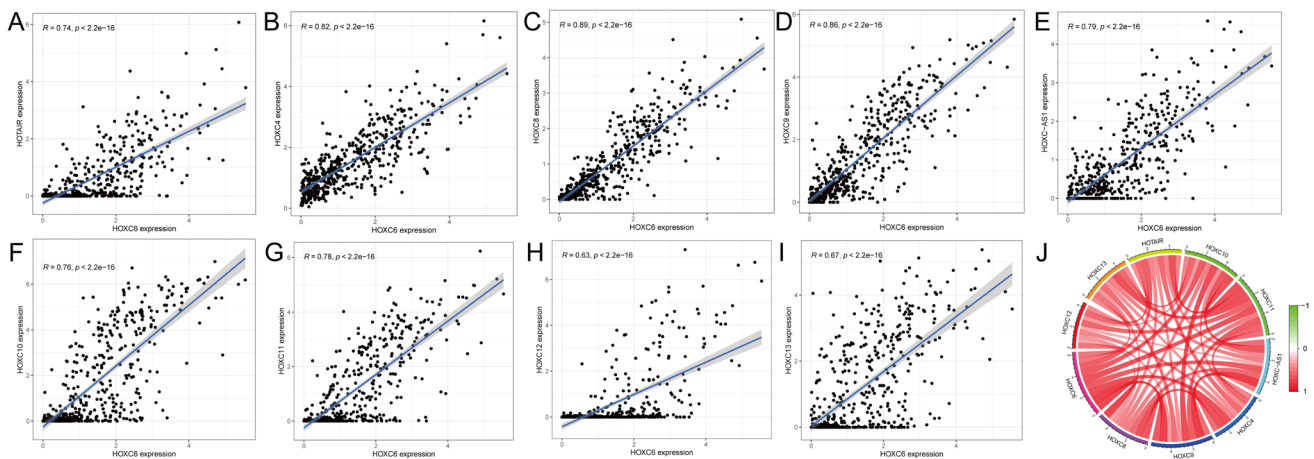
In the genome-wide correlation analysis on TCGA-LUAD dataset, the top 10 genes, including HOX antisense RNA (HOTAIR), HOXC4, HOXC8, HOXC9, HOXC-AS1, HOXC10, HOXC11, HOXC12, and HOXC13, were found to be positively relevant to HOXC6 (Fig. 4A–J). Furthermore, on the condition that the P-value < 0.001, we demonstrated that HOXC6 expressions were positively connected to several immune checkpoint-related genes, including CD200, CD276, TNFSF4, and TNFRSF4, and TMB (Figure S3A–C).
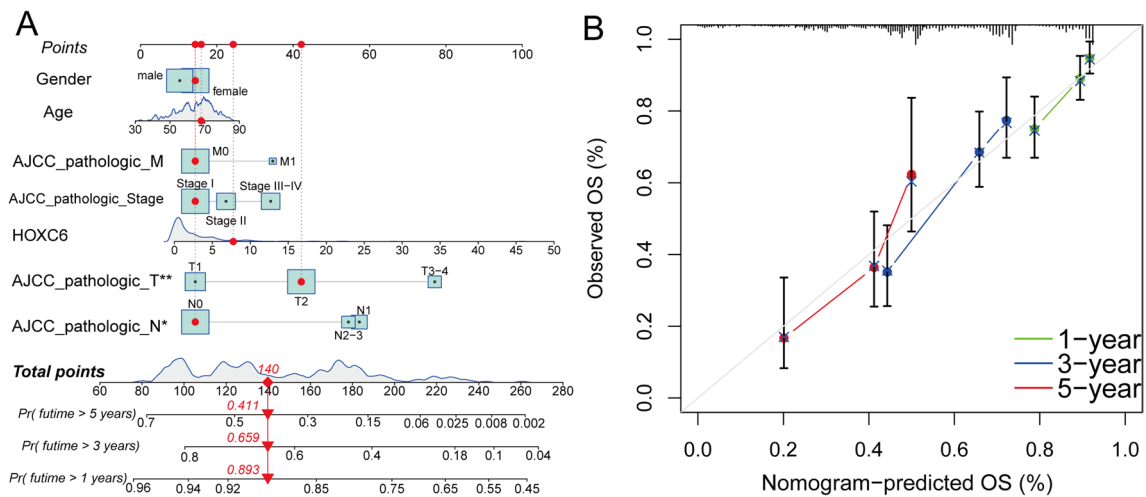
Fig. 3 **A** An established nomogram integrating the HOXC6 expression with readily available clinicopathological traits can be used to predict the 1-, 3-, and 5-year OS of TCGA-LUAD patients in clinical practice. **B** As a test of the nomogram, the calibration curves illustrated an acceptable degree of coherence between the projected and the actual OS rates at 1, 3, and 5 years. HOXC6, Homeobox C6; LUAD, Lung Adenocarcinoma; TCGA, The Cancer Genome Atlas; TNM, Tumor Node Metastasis; OS, overall survival

Fig. 4 **A–J** In the genome-wide correlation analysis on TCGA-LUAD dataset, the top 10 genes, including HOTAIR, HOXC4, HOXC8, HOXC9, HOXC-AS1, HOXC10, HOXC11, HOXC12, and HOXC13, were found to be positively relevant to HOXC6 and the results were summarized in a circus plot. HOXC6, Homeobox C6; LUAD, Lung Adenocarcinoma; TCGA, The Cancer Genome Atlas; HOTAIR, HOX antisense RNA

3.6 Correlation between HOXC6 and the immune infiltration of tumor microenvironment in LUAD

In CIBERSORT analysis, we revealed that HOXC6 expression was positively correlated to the infiltration levels of Macrophages M0, Plasma cells, NK cells resting, and T cells regulatory (Tregs), but was negatively associated with the Dendritic cells resting, Macrophages M2, Mast cells resting, Monocytes, NK cells activated, and T cells CD4 memory resting levels (Fig. 5A–J). The above correlation results were further summarized in a lollipop chart (Fig. 5K). In addition, Plasma cells, T cells regulatory (Tregs), and Macrophages M0 had a higher infiltration levels in the high-HOXC6 expression subgroup, while NK cells activated, Monocytes, Dendritic cells resting, Mast cells resting had the relatively lower infiltration levels (Fig. 5L). Moreover, there was a lower immune score in the high HOXC6 expression subgroup (Fig. 5M).
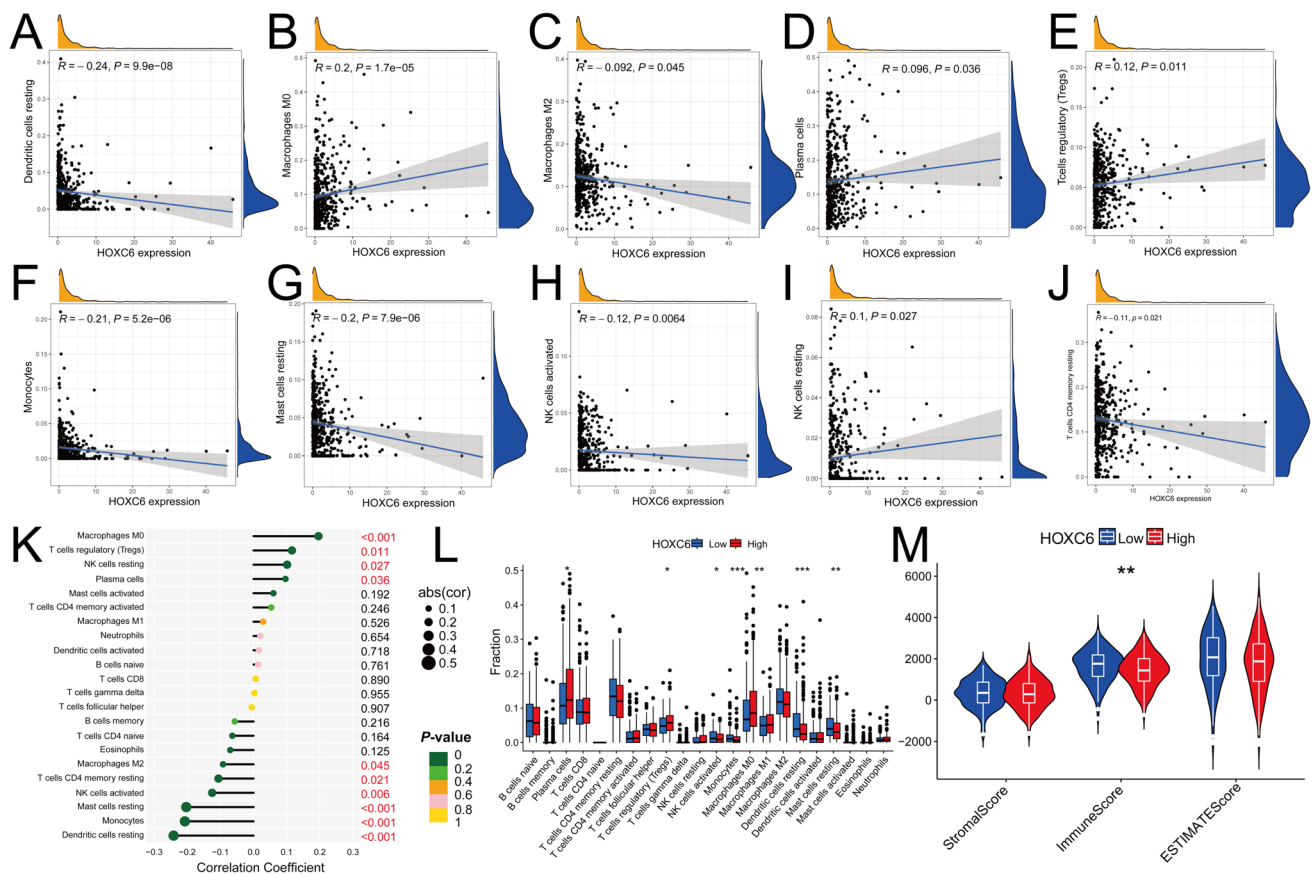
Discover

Fig. 5 **A–J** In CIBERSORT analysis, HOXC6 expression was positively correlated to the infiltration levels of Macrophages M0, Plasma cells, NK cells resting, and Tregs, but was negatively associated with the Dendritic cells resting, Macrophages M2, Mast cells resting, Monocytes, NK cells activated, and T cells CD4 memory resting levels in TCGA-LUAD dataset. **K** The results of correlation analysis between HOXC6 expression and the infiltration levels were further summarized in the lollipop chart. **L** In the high-HOXC6 expression subgroup, Plasma cells, Tregs, and Macrophages M0 had a higher infiltration levels, while NK cells activated, Monocytes, Dendritic cells resting, Mast cells resting had a relatively lower infiltration level. **M** A lower immune score was observed in the high HOXC6 expression subgroup. *$P < 0.05$; **$P < 0.01$; ***$P < 0.001$. CIBERSORT, cell-type identification by estimating relative subsets of RNA transcripts; HOXC6, Homeobox C6; LUAD, Lung Adenocarcinoma; TCGA, The Cancer Genome Atlas; Tregs, T cells regulatory

3.7 Predictive value of HOXC6 to therapeutic efficacy of medicines for LUAD patients

Based on the estimated medicine IC50 values, we demonstrated that eight medications (Camptothecin, Cytarabine, Docetaxel, Elesclomol, Rapamycin, Sorafinib, Temsirolimus, and Vorinostat) displayed a lower IC50s in the high-HOXC6 expression subgroup, which suggested that the LUAD patients with high- HOXC6 expression may be more susceptible to these medicines (Fig. 6A–H). Significantly, violin plots showed the low-HOXC6 expression subgroup exhibited a relatively higher IPS of CTLA4_negtive_PD-1_positive and CTLA4_postive_PD-1_positive, which represented that they may carry a favorable reaction to immunotherapy of PD-1 inhibitors, instead of CTLA-4 inhibitors (Fig. 6I–L).

4 Discussion

Molecular mechanisms of LUAD development can manifest as epigenetic alterations, genetic mutations, including Epidermal Growth Factor Receptor (EGFR), KRAS, and anaplastic lymphoma kinase (ALK), and chromosomal rearrangements [22–25]. In addition to conventional surgery and chemotherapy, the emerging targeted therapy and immunotherapy play an increasingly important role in the conversion, neoadjuvant and postoperative adjuvant therapy for
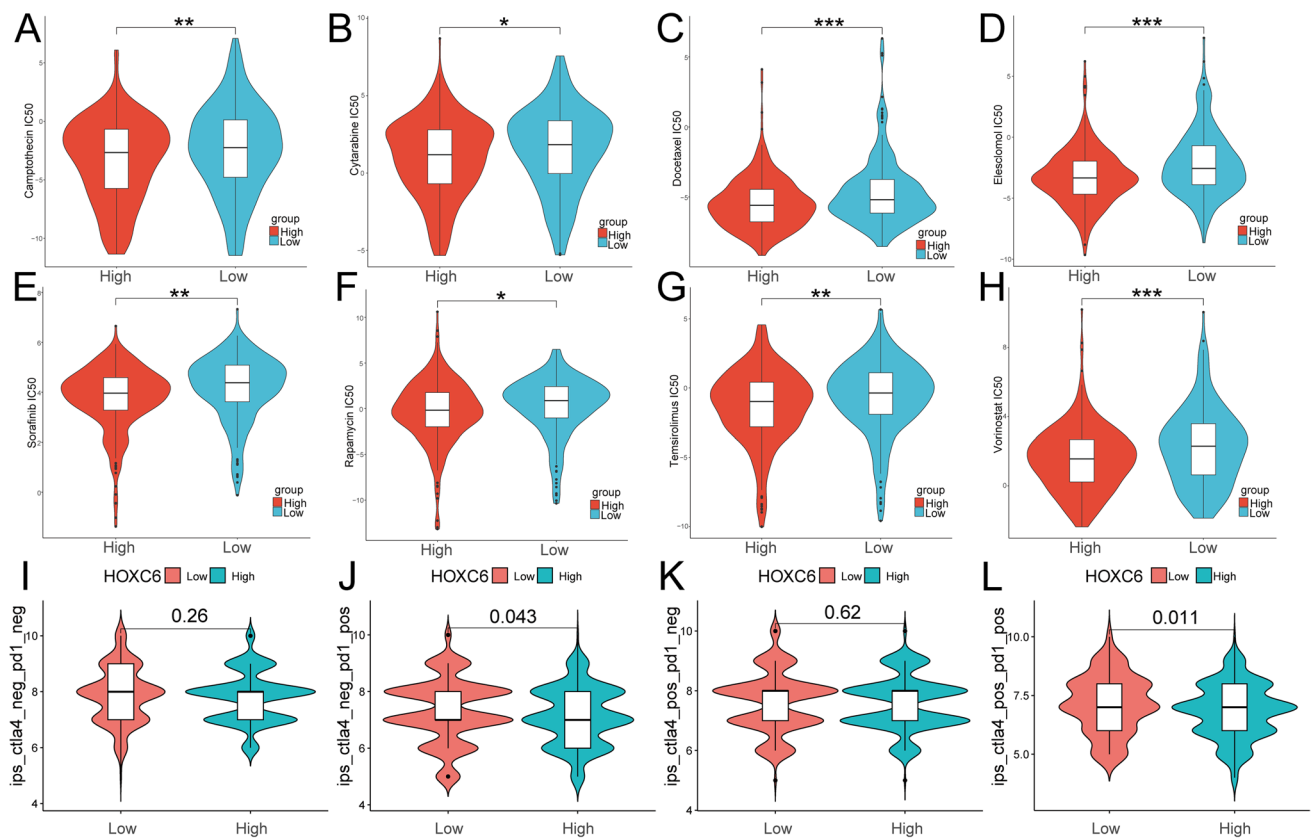
Fig. 6 **A**–**H** Eight medications (Camptothecin, Cytarabine, Docetaxel, Elesclomol, Rapamycin, Sorafinib, Temsirolimus, and Vorinostat) displayed a lower IC50s in the high-HOXC6 expression subgroup. **I**–**L** Violin plots showed the low-HOXC6 expression subgroup exhibited relatively higher IPS of CTLA4_negtive_PD-1_positive and CTLA4_postive_PD-1_positive. *$P < 0.05$; **$P < 0.01$; ***$P < 0.001$. HOXC6, Homeobox C6; IC50, half-maximal inhibitory concentration; immunophenotypic score (IPS); PD-1, programmed cell death protein-1; CTLA-4, cytotoxic T lymphocyte antigen-4

LUAD [26, 27]. Nevertheless, the treatment response for LUAD is full of challenges due to tumor heterogeneity and drug resistance, which may be induced by novel gene variants, Oncogenic pathway activation and the alteration of immune escape mechanisms [23, 28, 29]. Hence, identifying the immunologically relevant and prognostic biological marker for LUAD makes sense in improving the therapeutic effect of systemic combination treatment regimen. The previous study has proved the upregulated expression and carcinogenic properties of HOXC6 in NSCLC. Our study focused on the same common lung cancer, LUAD. Consistently, the dysregulated HOXC6 expression level was demonstrated in LUAD and was associated with advanced tumor status, which suggested that HOXC6 can serve as a prognostic biomarker for LUAD.

It was demonstrated that HOXC6/miR-188-5p axis has the potential to promote malignancy via preventing the FOXN2 signaling pathway from being activated [30]. Epithelial-mesenchymal transition (EMT), a cellular process by which cancer cells acquire invasive properties, could be a crucial approach that HOXC6 promotes cancer progression [31, 32]. In colorectal cancer, the interactive effect of cancer cells and Macrophages M2 induces EMT, which could be further promoted by IL6/HOXC6/DKK1/β-catenin signal pathway [32]. The previous study also underscored that HOXC6 may modulate the EMT signaling pathway and was related to tumor immune microenvironment in the development of gliomas [31]. In NSCLC, thymidylate synthase was significantly associated with EMT occurrence, in which HOXC6 and HMGA2 may serve as the upstream regulator [33]. In addition, it is demonstrated that HOXC6 was over-expressed in CRC and its upregulation was related to the higher infiltration levels of multiple immune cells, including Treg cells, CD68^{+} macrophages, CD66b^{+} neutrophils, and CD8^{+} T-cells, and increased PD-L1 and PD-1 expression levels [34]. Our results revealed up-regulated HOXC6 expression related to high T cells regulatory (Tregs) and Macrophages M0 cells infiltration levels. The ability to generate and recruit suppressive immune cells, such as tumor-associated macrophages (TAMs) and Treg cells, in the tumor microenvironment (TME) is one of the immune escape mechanisms of LUAD [35, 36]. TAMs can inhibit the activity of T cells by expressing PD-L1 and other immune checkpoint molecules and inducing the Tregs differentiation [37, 38].

It was discovered that drug-resistant cells overexpress the HOXC6 gene and HOXC6 activated MDR-1 (multidrug resistance) promoter activity, which resulted in chemotherapeutic drug resistance [39]. Gefitinib, a typical tyrosine kinase inhibitor (TKI) aiming at EGFR, is a targeted medicine to treat NSCLC. It is demonstrated that, for NSCLC patients with drug resistance to Gefitinib, HOXC6 could serve as a viable therapeutic targeting [40]. In our study, we also uncovered that the drug sensitivities of multiple common chemotherapeutic and targeted medicines were linked to HOXC6 expression, which may help with the decision-making of LUAD managements. Targeting HOXC6 may makes sense in inhibiting LUAD development and breaking drug resistance. But further research in vitro and in vivo is needed to fully elucidate the innate mechanisms.

5 Conclusions

Overall, HOXC6 can serve as prognostic biomarker for LUAD. Furthermore, it may be link to an immunosuppressive TME and have the potential to be an underlying therapeutic target for LUAD patients. What's more, more in-depth studies and investigations into carcinogenic property and clinical application of HOXC6 are in demand.

Declarations

References

1. Leiter A, Veluswamy RR, Wisnivesky JP. The global burden of lung cancer: current status and future trends. Nat Rev Clin Oncol. 2023;20(9):624–39. https://doi.org/10.1038/s41571-023-00798-3.
2. Sung H, Ferlay J, Siegel RL, Laversanne M, Soerjomataram I, Jemal A, et al. Global cancer statistics 2020: GLOBOCAN estimates of incidence and mortality worldwide for 36 cancers in 185 Countries. CA Cancer J Clin. 2021;71(3):209–49. https://doi.org/10.3322/caac.21660.
3. Wang MQ, Yin QY, Chen YR, Zhu SL. Diagnostic and prognostic value of HOXC family members in gastric cancer. Future Oncol. 2021;17(35):4907–23. https://doi.org/10.2217/fon-2021-0291.
4. Yang Y, Tang X, Song X, Tang L, Cao Y, Liu X, et al. Evidence for an oncogenic role of HOXC6 in human non-small cell lung cancer. PeerJ. 2019;7: e6629. https://doi.org/10.7717/peerj.6629.

5. Wang X, Chan S, Chen J, Xu Y, Dai L, Han Q, et al. Robust machine-learning based prognostic index using cytotoxic T lymphocyte evasion genes highlights potential therapeutic targets in colorectal cancer. Cancer Cell Int. 2024;24(1):52. https://doi.org/10.1186/s12935-024-03239-y.

6. Yazbek Hanna M, Winterbone M, O'Connell SP, Olivan M, Hurst R, Mills R, et al. Gene-transcript expression in urine supernatant and urine cell-sediment are different but equally useful for detecting prostate cancer. Cancers. 2023. https://doi.org/10.3390/cancers15030789.

7. Luo Z, Farnham PJ. Genome-wide analysis of HOXC4 and HOXC6 regulated genes and binding sites in prostate cancer cells. PLoS ONE. 2020;15(2): e0228590. https://doi.org/10.1371/journal.pone.0228590.

8. Malvi P, Chava S, Cai G, Hu K, Zhu LJ, Edwards YJK, et al. HOXC6 drives a therapeutically targetable pancreatic cancer growth and metastasis pathway by regulating MSK1 and PPP2R2B. Cell Reports Med. 2023;4(11): 101285. https://doi.org/10.1016/j.xcrm.2023.101285.

9. Steens J, Unger K, Klar L, Neureiter A, Wieber K, Hess J, et al. Direct conversion of human fibroblasts into therapeutically active vascular wall-typical mesenchymal stem cells. Cellular Mol Life Sci. 2020;77(17):3401–22. https://doi.org/10.1007/s00018-019-03358-0.

10. Wang X, Liao X, Yu T, Gong Y, Zhang L, Huang J, et al. Analysis of clinical significance and prospective molecular mechanism of main elements of the JAK/STAT pathway in hepatocellular carcinoma. Int J Oncol. 2019;55(4):805–22. https://doi.org/10.3892/ijo.2019.4862.

11. Livak KJ, Schmittgen TD. Analysis of relative gene expression data using real-time quantitative PCR and the 2(-Delta Delta C(T)) method. Methods. 2001;25(4):402–8. https://doi.org/10.1006/meth.2001.1262.

12. Zhou X, Li TM, Luo JZ, Lan CL, Wei ZL, Fu TH, et al. CYP2C8 Suppress proliferation, migration, invasion and Sorafenib resistance of hepatocellular carcinoma via PI3K/Akt/p27(kip1) axis. J Hepatocellular Carcinoma. 2021;8:1323–38. https://doi.org/10.2147/jhc.S335425.

13. Xie H, Yang K, Qin C, Zhou X, Liu J, Nong J, et al. Sarcosine dehydrogenase as an immune infiltration-associated biomarker for the prognosis of hepatocellular carcinoma. J Cancer. 2024;15(1):149–65. https://doi.org/10.7150/jca.89616.

14. FE HJ. rms: regression modeling strategies. R package version 6.7–0. 2023. https://CRAN.R-project.org/package=rms

15. TM T. survival: survival analysis. R package version 3.5–7. 2023. https://CRAN.R-project.org/package=survival

16. Li L, Li J. Correlation of tumor mutational burden with prognosis and immune infiltration in lung adenocarcinoma. Front Oncol. 2023;13:1128785. https://doi.org/10.3389/fonc.2023.1128785.

17. Subramanian A, Kuehn H, Gould J, Tamayo P, Mesirov JP. GSEA-P: a desktop application for gene set enrichment analysis. Bioinformatics. 2007;23(23):3251–3. https://doi.org/10.1093/bioinformatics/btm369.

18. Newman AM, Liu CL, Green MR, Gentles AJ, Feng W, Xu Y, et al. Robust enumeration of cell subsets from tissue expression profiles. Nat Methods. 2015;12(5):453–7. https://doi.org/10.1038/nmeth.3337.

19. Yoshihara K, Shahmoradgoli M, Martínez E, Vegesna R, Kim H, Torres-Garcia W, et al. Inferring tumour purity and stromal and immune cell admixture from expression data. Nat Commun. 2013;4:2612. https://doi.org/10.1038/ncomms3612.

20. Geeleher P, Cox N, Huang RS. pRRophetic: an R package for prediction of clinical chemotherapeutic response from tumor gene expression levels. PLoS ONE. 2014;9(9): e107468. https://doi.org/10.1371/journal.pone.0107468.

21. Charoentong P, Finotello F, Angelova M, Mayer C, Efremova M, Rieder D, et al. Pan-cancer immunogenomic analyses reveal genotype-immunophenotype relationships and predictors of response to checkpoint blockade. Cell Rep. 2017;18(1):248–62. https://doi.org/10.1016/j.celrep.2016.12.019.

22. Gallina FT, Tajè R, Letizia Cecere F, Forcella D, Landi L, Minuti G, et al. ALK rearrangement is an independent predictive factor of unexpected nodal metastasis after surgery in early stage, clinical node negative lung adenocarcinoma. Lung Cancer. 2023;180: 107215. https://doi.org/10.1016/j.lungcan.2023.107215.

23. Liang J, Bi G, Sui Q, Zhao G, Zhang H, Bian Y, et al. Transcription factor ZNF263 enhances EGFR-targeted therapeutic response and reduces residual disease in lung adenocarcinoma. Cell Rep. 2024;43(2): 113771. https://doi.org/10.1016/j.celrep.2024.113771.

24. Kuhlmann-Hogan A, Cordes T, Xu Z, Kuna RS, Traina KA, Robles-Oteíza C, et al. EGFR-driven lung adenocarcinomas Co-opt alveolar macrophage metabolism and function to support EGFR signaling and growth. Cancer Discov. 2024. https://doi.org/10.1158/2159-8290.Cd-23-0434.

25. Wang J, Dong L, Zheng Z, Zhu Z, Xie B, Xie Y, et al. Effects of different KRAS mutants and Ki67 expression on diagnosis and prognosis in lung adenocarcinoma. Sci Rep. 2024;14(1):4085. https://doi.org/10.1038/s41598-023-48307-x.

26. Wang X, Meng X, Cai G, Jin P, Bai M, Fu Y, et al. Survival outcomes of targeted and immune consolidation therapies in locally advanced unresectable lung adenocarcinoma. Int Immunopharmacol. 2024;129: 111684. https://doi.org/10.1016/j.intimp.2024.111684.

27. Yang H, Ma W, Sun B, Fan L, Xu K, Hall SSR, et al. Smoking signature is superior to programmed death-ligand 1 expression in predicting pathological response to neoadjuvant immunotherapy in lung cancer patients. Translat Lung Cancer Res. 2021;10(9):3807–22. https://doi.org/10.21037/tlcr-21-734.

28. Xu H, Du Z, Li Z, Liu X, Li X, Zhang X, et al. MUC1-EGFR crosstalk with IL-6 by activating NF-κB and MAPK pathways to regulate the stemness and paclitaxel-resistance of lung adenocarcinoma. Ann Med. 2024;56(1):2313671. https://doi.org/10.1080/07853890.2024.2313671.

29. Sui Q, Hu Z, Jin X, Bian Y, Liang J, Zhang H, et al. The genomic signature of resistance to platinum-containing neoadjuvant therapy based on single-cell data. Cell Biosci. 2023;13(1):103. https://doi.org/10.1186/s13578-023-01061-z.

30. Jeong S, Kim SA, Ahn SG. HOXC6-mediated miR-188–5p expression induces cell migration through the inhibition of the tumor suppressor FOXN2. Int J Mol Sci. 2021. https://doi.org/10.3390/ijms23010009.

31. Huang H, Huo Z, Jiao J, Ji W, Huang J, Bian Z, et al. HOXC6 impacts epithelial-mesenchymal transition and the immune microenvironment through gene transcription in gliomas. Cancer Cell Int. 2022;22(1):170. https://doi.org/10.1186/s12935-022-02589-9.

32. Qi L, Chen J, Zhou B, Xu K, Wang K, Fang Z, et al. HomeoboxC6 promotes metastasis by orchestrating the DKK1/Wnt/β-catenin axis in right-sided colon cancer. Cell Death Dis. 2021;12(4):337. https://doi.org/10.1038/s41419-021-03630-x.

33. Siddiqui MA, Gollavilli PN, Ramesh V, Parma B, Schwab A, Vazakidou ME, et al. Thymidylate synthase drives the phenotypes of epithelial-to-mesenchymal transition in non-small cell lung cancer. Br J Cancer. 2021;124(1):281–9. https://doi.org/10.1038/s41416-020-01095-x.

34. Weng M, Lai Y, Ge X, Gu W, Zhang X, Li L, et al. HOXC6: a promising biomarker linked to an immunoevasive microenvironment in colorectal cancer based on TCGA analysis and cohort validation. Heliyon. 2024;10(1): e23500. https://doi.org/10.1016/j.heliyon.2023.e23500.

35. Hu Z, Sui Q, Jin X, Shan G, Huang Y, Yi Y, et al. IL6-STAT3-C/EBPβ-IL6 positive feedback loop in tumor-associated macrophages promotes the EMT and metastasis of lung adenocarcinoma. J Exp Clin Cancer Res. 2024;43(1):63. https://doi.org/10.1186/s13046-024-02989-x.

Discover

36. Zeng Z, Du W, Yang F, Hui Z, Wang Y, Zhang P, et al. The spatial landscape of T cells in the microenvironment of stage III lung adenocarcinoma. J Pathol. 2024. https://doi.org/10.1002/path.6254.

37. Huang Z, Xiao Z, Yu L, Liu J, Yang Y, Ouyang W. Tumor-associated macrophages in non-small-cell lung cancer: from treatment resistance mechanisms to therapeutic targets. Crit Rev Oncol Hematol. 2024;196: 104284. https://doi.org/10.1016/j.critrevonc.2024.104284.

38. Ji S, Shi Y, Yin B. Macrophage barrier in the tumor microenvironment and potential clinical applications. Cell Commun Signal. 2024;22(1):74. https://doi.org/10.1186/s12964-023-01424-6.

39. Kim KJ, Moon SM, Kim SA, Kang KW, Yoon JH, Ahn SG. Transcriptional regulation of MDR-1 by HOXC6 in multidrug-resistant cells. Oncogene. 2013;32(28):3339–49. https://doi.org/10.1038/onc.2012.354.

40. He W, Qin M, Cai Y, Gao X, Cao S, Wang Z, et al. Downregulation of HOXC6 by miR-27a ameliorates gefitinib resistance in non-small cell lung cancer. Am J Cancer Res. 2021;11(9):4329–46.